Astron. Astrophys. 345, 915–924 (1999)

ASTRONOMY AND ASTROPHYSICS

# Probing the Na I D and K I λ7699 resonance lines sensitivity to background opacity in late-type stars⋆

**A. Tripicchio[1], M.T. Gomez[1], G. Severino[1], E. Covino[1], R.J. García López[2], and L. Terranegra[1]**

[1] Osservatorio Astronomico di Capodimonte, Via Moiariello 16, I-80131 Naples, Italy
[2] Instituto de Astrofísica de Canarias, E-38200 La Laguna, Tenerife, Spain

Received 16 November 1998 / Accepted 19 March 1999

**Abstract.** We have measured the equivalent width $W_{\rm K}$ of the K I resonance line at 7699 Å for a large sample of low activity late-type stars observed with high spectral resolution and we have verified that the relation $W_{\rm K}$ vs. $T_{\rm eff}$ is monotonically decreasing, for both dwarf and giant stars. This behaviour is different from that of the Na I D lines for stars of the same type, which showed that the relation $W_{\rm Na}$ vs. $T_{\rm eff}$ has a maximum for $T_{\rm eff} \sim 4000$ K, which is better defined for giants than for dwarfs (Tripicchio et al. 1997).

The fit of the observed K I equivalent widths by means of a NLTE spectral line synthesis using conventional background opacity shows that, for dwarf stars, the adopted models overestimate the observed $W_{\rm K}$ for temperatures $\lesssim 4000$ K. This result is similar to that discussed for the Na I D lines in our previous paper. On the other hand, for giant stars with $T_{\rm eff} \lesssim 3800$ K these models in general underestimate $W_{\rm K}$.

The discrepancies between observed and computed $W_{\rm K}$ and $W_{\rm Na}$ for cool stars are much stronger than the variations due to uncertainties in either atmospheric model or line parameters, like effective temperature and surface gravity, or Van der Waals broadening. For M dwarf stars, the most convincing explanation for the disagreement is the lack of atomic and molecular line opacity in the adopted models. In fact, a NLTE spectral synthesis including an additional background opacity reproduces with a good level of accuracy the equivalent widths, as well as the general shape of the profiles for both the Na I D and K I lines, in a subsample of early-M dwarfs.

**Key words:** stars: late-type – stars: atmospheres – line: formation – radiative transfer – line: profiles

## 1. Introduction

In a previous work, Tripicchio et al. (1997, hereafter T97) have tested current models of late-type stellar atmospheres (including photosphere and low chromosphere) using the equivalent width of the D resonance lines of neutral sodium, $W_{\rm Na}$, as a diagnostic. They found that the observed $W_{\rm Na}$ vs. effective temperature, $T_{\rm eff}$, relation, had a maximum for $T_{\rm eff} \sim 4000$ K, and that the adopted model atmospheres were able to reproduce the observations for stars with $T_{\rm eff}$ greater than $\sim 4000$K, while overestimated $W_{\rm Na}$ in cooler stars. This discrepancy was too large to be due to uncertainties in effective temperature, surface gravity, sodium abundance or microturbulence.

In the present work the observational dataset of T97 has been extended to another alkali resonance line, K I λ7699. In fact, as suggested recently by Severino et al. (1994) and Montes & Martin (1998), both Na I and K I resonance lines can be included in a set of spectral features useful for atmospheric studies from F to M dwarf stars, if properly treated as semiempirical diagnostics. The K I resonance line is weaker than the Na I D lines due to the smaller abundance of this element in solar-like stars. It is also well separated from the other line of the doublet (K I λ7667) and this fact, added to the larger interval covered by our observations in the red spectral band, allows a better determination of the observed local continuum level and hence of $W_{\rm K}$. Moreover the K I λ7699 line, only weakly affected by collisional broadening, has less pronounced Lorentzian wings than the Na I D lines.

In T97 the lack of atomic and molecular line opacity in the calculations was indicated as a possible explanation for the disagreement from observations. In recent literature many authors have dealt with the subject of modelling the atmospheric structure of M dwarfs facing the difficult treatment of opacity sources in cool stars. Allard & Hauschildt (1995) published the results of 700 photospheric models for cool stars calculated with the Phoenix code which included molecular opacities from TiO and $H_2O$ sources. More recently Allard et al. (1997) have incorporated molecular and grain opacities in cool stellar spectra deriving the effective temperature scale for M dwarfs and a new grid of model atmospheres and synthetic spectra for brown dwarfs. Andretta et al. (1997) studied the dependence on chromospheric activity in M dwarfs of the D lines compared with hydrogen spectrum, including a proper treatment of background opacities in Carlsson (1986) code, with improved molecular sources from the Phoenix photospheric package. Short & Doyle (1997) presented NLTE calculations of the H I spectrum in a grid of chromospheric models that represents a dM0 star and investi-

*Send offprint requests to*: A. Tripicchio

⋆ Based on observations collected at the European Southern Observatory (ESO), La Silla, Chile, and at the McDonald Observatory, Mt. Locke, Texas, USA

*Correspondence to*: tripicchio@na.astro.it

gated three different treatments of background opacity: continuum opacity only, blanketing due to lines that form in the photosphere below the temperature minimum, and blanketing by lines that form throughout the entire atmosphere. Mauas et al. (1997) computed models for M dwarf stars with the program Pandora (Avrett et al. 1986), including line opacity computed by Kurucz (1991); moreover for each line studied in detail they modified the background opacities around it in order to match the observed continuum intensity. More recently Short & Doyle (1998) investigated the effect of including line blanketing opacity in Na D lines NLTE calculations, in order to fit high resolution spectra of five M dwarfs of low to high activity level. Generation of large databases for frequency average opacity is a natural by-product of these studies.

We are aware of the necessity of a proper numerical treatment of the background opacity, if one wants to produce model line profiles which match observations in detail. However, in order to reproduce the Na I D and K I $\lambda$7699 line equivalent widths, in this work we find it is sufficient to include in the NLTE spectral synthesis an additional background opacity scaled on the $H^-$ absorption coefficient. This model of additional opacity is based on the work of Zwaan (1974), who introduced a wavelength dependent opacity enhancement factor to better reproduce the observed continuum intensity of solar spots. Our approach is based on the remark that the Na I D and K I $\lambda$7699 features observed by us in M dwarfs are similar to the corresponding line profiles observed in high-resolution spectra of solar spots by Brynildsen et al. (1993) and reported by Caccin et al. (1993).

The present paper is structured as follows: in Sect. 2 we present the observational data and the measurements of the equivalent width of the K I $\lambda$7699 line in a large sample of late-type stars; in Sect. 3 we describe the atmospheric and opacity models used for the spectral synthesis; in Sect. 4 we compare observed and calculated $W_K$ for all the stars in our sample, as well as the Na and K line profiles in a selected number of M dwarfs; in Sect. 5 we summarize the results and draw our main conclusions.

## 2. Observations and data analysis

High-resolution spectra of the K I $\lambda$7699 line for 32 dwarf and 41 giant late-type stars with low activity have been obtained during three different observing runs (between 1994 and 1997), using the 1.4-m Coudé Auxiliary Telescope (CAT) feeding the Coudé Echelle Spectrometer (CES) of the European Southern Observatory (ESO) at La Silla (Chile), and with the 2.7-m telescope of McDonald Observatory (Texas), also equipped with a coudé echelle spectrograph.

Table 1 lists the observed stars; the spectral type is given in Column 2, the $V$ magnitude in Column 3, the observing run in Column 4, the exposure time in Column 5, the signal to noise ratio S/N in Column 6, and the measured equivalent line widths $W_K$ in Column 7.

The CAT observations were carried out in remote control from ESO headquarters in Garching during two observing runs: 1995 March 12–16, and 1997 July 10–14. In 1995, the LORAL UV-coated ESO CCD #34 was used. In 1997, the LORAL/LESSER UV-flooded ESO CCD #38 was used. In both cases, the CES was operated in the long camera configuration (Kaper & Pasquini 1996).

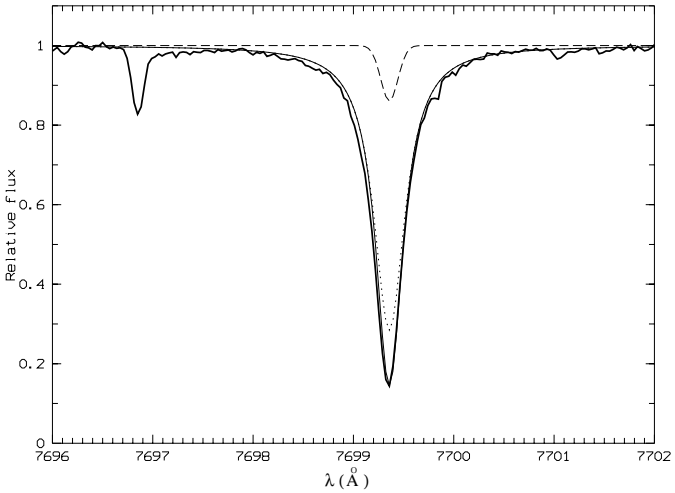


**Fig. 1.** Fit of the K I $\lambda$7699 line used to measure $W_K$ for HD156026. Thick solid line: observed profile; thin solid line: fitted profile; dotted: Lorentzian contribution to the fit; dashed: Gaussian contribution.

The spectral range covered was about 90 Å, from 7660 to 7750 Å, centred on the K I line. An entrance slit of 454 $\mu$m, corresponding to about 2 arcsec on the sky, was used yielding a nominal resolving power $\lambda/\Delta\lambda \sim 60000$. The exposure times ranged from 30 s, for 2.2 mag stars, up to 1 h, for 10.0 mag stars, typically the M dwarf stars. The achieved S/N was $\sim 430$ in the average, and less than 100 only for three spectra. The wavelength calibration and the flat-fielding were done as in T97. The data reduction was performed with the MIDAS[1] package using the long-slit context following the standard procedure of bias subtraction, flat-fielding, and wavelength calibration. See T97 for a detailed description of the observations obtained at McDonald.

To determine the line equivalent widths, the K I line profile has been fitted with an approximated Voigt function, i.e. the superposition of a Lorentzian and a Gaussian. Fig. 1 shows, as an example, the fit for HD156026, and the contribution to the fit of the two terms. In order to avoid a systematic overestimation of $W_K$, the numerous blends present in the wings of the K I line have been carefully excluded from the fit. The equivalent width, $W_K$, has then been measured by means of a linear integration of the fitted function. The error associated with $W_K$ has been estimated by relaxing the condition that the continuum level is equal to 1, and by repeating the fit and the integration. Errors range typically between a few mÅ and about 65 mÅ for the coolest stars, because the uncertainty on the location of the

[1] MIDAS is distributed by ESO and the versions 92NOV and 95NOV, used by us for the reductions, are available at the Osservatorio Astronomico di Capodimonte.

**Table 1.** List of the observed stars.

| HD # | Sp. type | $V$ mag | Obs. run | Exp. s | S/N | $W_{\rm K}$ mÅ |
|---|---|---|---|---|---|---|
| 28 | K0 III | 4.61 | McD 94 | 300 | 470 | 229 |
| | | | | 300 | 480 | 224 |
| | | | | 300 | 450 | 206 |
| 693 | F5 V | 4.90 | CAT 97 | 3600 | 590 | 137 |
| 1014 | M3 III | 5.12 | McD 94 | 300 | 700 | 430 |
| | | | | 300 | 670 | 442 |
| | | | | 300 | 590 | 426 |
| 1522 | K1.5 III | 3.50 | CAT 97 | 600 | 580 | 240 |
| 1581 | F9 V | 4.19 | CAT 97 | 900 | 440 | 142 |
| 1835 | G2.5 V | 6.38 | McD 94 | 1200 | 350 | 210 |
| | | | | 1200 | 300 | 212 |
| | | | | 1200 | 350 | 208 |
| 1879 | M2 III | 6.45 | McD 94 | 1200 | 660 | 359 |
| | | | | 1200 | 670 | 338 |
| | | | | 1200 | 590 | 381 |
| 3302 | F6 V | 5.50 | CAT 97 | 1200 | 250 | 158 |
| 4391 | G1 V | 4.79 | CAT 97 | 900 | 250 | 160 |
| 4408 | M4 III | 5.35 | McD 94 | 240 | 640 | 488 |
| | | | | 240 | 650 | 501 |
| | | | | 240 | 630 | 479 |
| 4656 | K4.5 III | 4.43 | McD 94 | 200 | 560 | 332 |
| | | | | 200 | 580 | 332 |
| | | | | 200 | 580 | 320 |
| 5756 | G3 III | 7.43 | CAT 97 | 1800 | 190 | 157 |
| 6805 | K2 III | 3.45 | McD 94 | 180 | 670 | 282 |
| | | | | 180 | 690 | 253 |
| | | | | 180 | 690 | 257 |
| 9270 | G7 III | 3.62 | McD 94 | 150 | 550 | 235 |
| | | | | 150 | 570 | 228 |
| | | | | 150 | 560 | 240 |
| 10700 | G8 V | 3.50 | McD 94 | 120 | 460 | 202 |
| | | | | 120 | 470 | 228 |
| | | | | 120 | 460 | 228 |
| 10824 | K4 III | 5.30 | CAT 97 | 1200 | 460 | 251 |
| 12274 | M0 III | 4.00 | McD 94 | 180 | 660 | 350 |
| | | | | 180 | 670 | 379 |
| | | | | 180 | 640 | 432 |
| 16160 | K3 V | 6.81 | McD 94 | 300 | 300 | 340 |
| | | | | 300 | 300 | 362 |
| | | | | 300 | 290 | 418 |
| 17925 | K1 V | 6.08 | CAT 97 | 2400 | 310 | 277 |
| 18322 | K1 III | 3.89 | McD 94 | 240 | 610 | 228 |
| | | | | 240 | 620 | 223 |
| | | | | 240 | 600 | 234 |
| | | | | 240 | 620 | 236 |
| 18884 | M1.5 III | 2.53 | McD 94 | 30 | 680 | 375 |
| | | | | 30 | 660 | 400 |
| | | | | 30 | 660 | 396 |
| 20630 | G5 V | 4.83 | McD 94 | 300 | 400 | 189 |
| | | | | 300 | 390 | 160 |
| | | | | 300 | 410 | 203 |
| 22049 | K2 V | 3.73 | McD 94 | 300 | 720 | 301 |
| | | | | 300 | 680 | 300 |
| | | | | 300 | 600 | 307 |
| 23940 | G6 III | 5.50 | CAT 97 | 1500 | 360 | 219 |
| 27808 | F8 V | 7.14 | McD 94 | 1200 | 270 | 154 |
| | | | | 1200 | 320 | 151 |
| | | | | 1800 | 270 | 156 |
| 36395 | M1.5 V | 7.92 | CAT 95 | 3600 | 180 | 980 |
| 42581 | M1.5 V | 8.14 | CAT 95 | 2700 | 90 | 917 |
| | | | | 2700 | 90 | 916 |
| 50281 | K3 V | 6.57 | CAT 95 | 1200 | 80 | 391 |
| 57615 | M3 III | 5.87 | CAT 95 | 1200 | 290 | 474 |
| 82668 | K5 III | 3.13 | CAT 95 | 600 | 460 | 266 |
| 84748 | M8 IIIe | 6.02 | CAT 95 | 1200 | 450 | 456 |

**Table 1.** (Continued)

| HD # | Sp. type | $V$ mag | Obs. run | Exp. s | S/N | $W_{\rm K}$ mÅ |
|---|---|---|---|---|---|---|
| 91214 | G5 III | 6.90 | CAT 97 | 1200 | 160 | 184 |
| 91848 | G2 III | 6.97 | CAT 97 | 1800 | 160 | 199 |
| 95578 | M0 III | 4.74 | CAT 95 | 1200 | 410 | 369 |
| 100623 | K0 V | 6.70 | CAT 97 | 1200 | 210 | 196 |
| 114613 | G3 V | 6.30 | CAT 97 | 1200 | 430 | 194 |
| 117287 | M7 IIIe | 4.97 | CAT 95 | 1200 | 280 | 534 |
| 117675 | M2.5 III | 4.69 | CAT 95 | 1200 | 420 | 385 |
| 119850 | M2 V | 8.46 | CAT 95 | 3600 | 120 | 853 |
| 120323 | M4.5 III | 4.19 | CAT 95 | 1200 | 360 | 598 |
| 120467 | K4.5 V | 8.16 | CAT 95 | 3600 | 110 | 595 |
| 122250 | M6.5 III | 5.48 | CAT 95 | 1200 | 380 | 577 |
| 124580 | F9 V | 6.30 | CAT 97 | 1200 | 220 | 152 |
| 131976 | M1.5 V | 8.10 | CAT 95 | 3600 | 160 | 994 |
| 131977 | K4 V | 8.10 | CAT 95 | 2700 | 160 | 413 |
| 133216 | M3.5 III | 3.29 | CAT 95 | 600 | 310 | 480 |
| 139084 | K0 V | 8.73 | CAT 97 | 3600 | 190 | 249 |
| | | | | 3600 | 150 | 284 |
| 150420 | G3 III | 7.15 | CAT 97 | 1200 | 280 | 170 |
| | | | | 3000 | 200 | 190 |
| 156026 | K5 V | 7.32 | CAT 97 | 1800 | 330 | 460 |
| 161096 | K2 III | 2.78 | CAT 97 | 300 | 620 | 260 |
| 163917 | G9 III | 3.28 | CAT 97 | 300 | 460 | 199 |
| 171443 | K3 III | 3.90 | CAT 97 | 300 | 420 | 266 |
| 176678 | K1 III | 4.00 | CAT 97 | 300 | 370 | 225 |
| 177241 | K0 III | 3.78 | CAT 97 | 300 | 420 | 209 |
| 191408 | K3 V | 5.96 | CAT 97 | 1200 | 380 | 268 |
| 197481 | M0 Ve | 10.03 | CAT 97 | 3600 | 180 | 740 |
| | | | | 3600 | 220 | 690 |
| 197692 | F5 V | 4.09 | CAT 97 | 600 | 340 | 141 |
| 198026 | M3 III | 4.40 | CAT 97 | 300 | 440 | 316 |
| 203608 | F6 V | 4.19 | CAT 97 | 600 | 360 | 117 |
| 204381 | K0 III | 4.50 | CAT 97 | 600 | 370 | 194 |
| 209100 | K4.5 V | 5.88 | CAT 97 | 900 | 460 | 387 |
| 209290 | M0.5 V | 9.16 | McD 94 | 1800 | 170 | 840 |
| | | | | 1800 | 140 | 851 |
| | | | | 1800 | 190 | 912 |
| | | | | 1800 | 210 | 824 |
| | | | | 1800 | 180 | 835 |
| | | | | 1800 | 200 | 830 |
| 211391 | G9 III | 4.16 | McD 94 | 200 | 490 | 239 |
| | | | | 240 | 540 | 237 |
| | | | | 240 | 550 | 239 |
| 214850 | G4 V | 5.71 | McD 94 | 300 | 250 | 167 |
| | | | | 900 | 460 | 163 |
| | | | | 900 | 480 | 170 |
| 214952 | M5 III | 2.20 | CAT 97 | 30 | 600 | 384 |
| 217580 | K4 V | 7.46 | McD 94 | 1800 | 290 | 312 |
| | | | | 1800 | 320 | 319 |
| | | | | 1800 | 310 | 318 |
| 218329 | M1 III | 4.52 | McD 94 | 300 | 740 | 366 |
| | | | | 300 | 730 | 402 |
| | | | | 300 | 750 | 394 |
| 218594 | K1.5 III | 3.66 | McD 94 | 180 | 600 | 254 |
| | | | | 180 | 580 | 253 |
| | | | | 180 | 590 | 242 |
| 219615 | G9 III | 3.70 | CAT 97 | 300 | 400 | 193 |
| 220096 | G4 V | 5.69 | CAT 97 | 3600 | 470 | 197 |
| 221148 | K3 III | 6.25 | McD 94 | 900 | 390 | 278 |
| | | | | 1500 | 500 | 250 |
| | | | | 1200 | 520 | 290 |
| 223719 | K4 III | 5.55 | McD 94 | 600 | 530 | 317 |
| | | | | 600 | 540 | 340 |
| 224935 | M3 III | 4.40 | McD 94 | 200 | 720 | 476 |
| | | | | 200 | 780 | 489 |
| | | | | 200 | 700 | 463 |

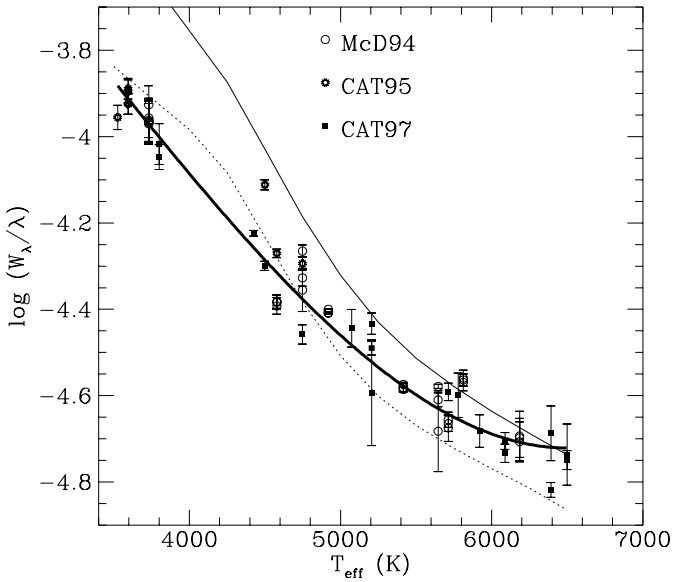


**Fig. 2.** Observed and calculated logarithm of $W_{\rm K}/\lambda$ vs. $T_{\rm eff}$ for dwarf stars. $W_{\rm K}$ is expressed in Å and $\lambda$= 7699 Å. The thick solid line refers to the fit given in Sect. 2.1. The thin solid and the dotted lines represent calculations (see Sect. 4.1) without and with additional opacity ($OF$=0 and $OF$=1.5), respectively.

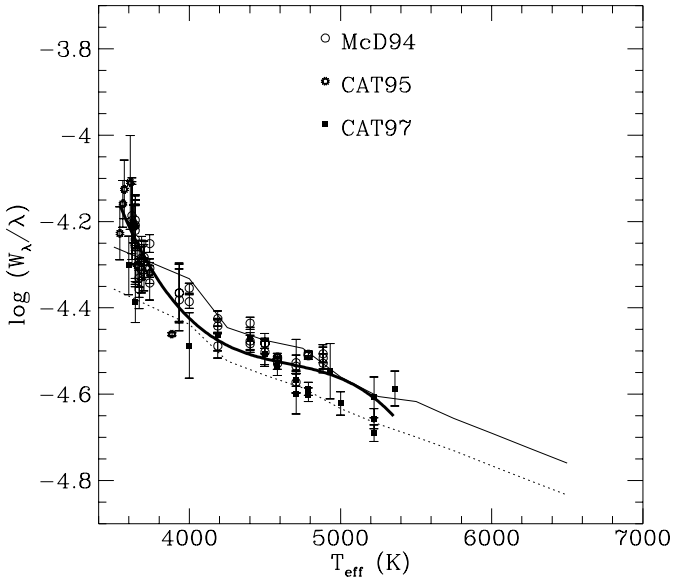


**Fig. 3.** Same as in Fig. 2, but for giant stars.

continuum is larger for these stars. The data analysis described above has been carried out with MIDAS.

### *2.1. Observed $W_{\rm K}$ vs. $T_{\rm eff}$*

The $W_{\rm K}$ measured in 56 spectra obtained for the 32 dwarf stars and in 74 spectra of the 41 giant stars, are plotted as a function of $T_{\rm eff}$, in Figs. 2 and 3, respectively. The effective temperatures of the sample stars have been derived from the $T_{\rm eff}$ vs. spectral type calibrations of Gray (1989), as in T97. In these calibrations, the absolute error on $T_{\rm eff}$ is about 300 K, and comparisons with other calibrations show that, for the coolest stars, it can reach a maximum of about 500 K (T97). The observed $W_{\rm K}$ increases for decreasing $T_{\rm eff}$, for both dwarf and giant stars, as expected, because the number of neutral potassium atoms increases at low effective temperatures. We note that the equivalent width measured on the K I $\lambda$7699 line in the spectrum of a sunspot umbra, i.e. $\log W_{\rm K}/\lambda = -3.83$, fits well to the low temperature trend for dwarf stars plotted in Fig. 2. The same agreement between solar spot and cool stellar dwarfs equivalent widths holds for the sodium doublet, which has a value of $\log W_{\rm Na}/\lambda = -2.63$ in the sunspot (see Fig. 6 in T97).

We have performed two weighted third order polynomial least squares fits, one for the observed dwarf stars, and the other for the giant stars. The relations obtained, and plotted in Figs. 2 and 3, are the following:

$$\log \frac{W_{\rm K}}{7699} = a_0 + a_1 T_{\rm eff} + a_2 T_{\rm eff}^2 + a_3 T_{\rm eff}^3 \qquad (1)$$

with $W_{\rm K}$ expressed in Å, and with $a_0$= −2.85, $a_1$= 3.29 $10^{-5}$, $a_2$= −1.43 $10^{-7}$, $a_3$= 1.44 $10^{-11}$, and $a_0$= 16.7, $a_1$= −1.3545 $10^{-2}$, $a_2$= 2.895 $10^{-6}$, $a_3$= −2.073 $10^{-10}$, for dwarfs and giants respectively. The standard deviation in $\log W_{\rm K}$ units is 0.05 in both cases. A second order fit would be sufficient as well, yielding a standard deviation of $\sim$ 0.06, while a first order fit does not accurately reproduce the trend. This relation can be inverted and used to determine $T_{\rm eff}$ with a dispersion of about $\pm$200 K. In particular, from this analysis, $W_{\rm K}$ appears to be a better temperature indicator for dwarf than for giants stars.

Note that for giants hotter than about $5400$K the K I line is no longer detectable, while for dwarfs the temperature upper limit is greater than $6400$K. In fact, for giant stars, the rotation boundary separating fast rotators (hotter stars) from slow rotators happens to be at later spectral type than for dwarf stars (Gray 1992). Thus, for example, giants with spectral type F8 would generally rotate faster than dwarfs of the same spectral type. This fact implies that in F8 and earlier giants, the K I line is so broad and shallow that we can hardly detect it. Actually, except for the F5 dwarf HD197692 and the F6 dwarf HD3302, for which $v \sin i \sim 50$ Km s$^{-1}$, the 22 sample stars in common with the catalogue of Uesugi & Fukuda (1982) have $v \sin i < 20$ Km s$^{-1}$.

## 3. Calculations

### *3.1. Model atmospheres*

We have adopted the temperature and electronic density height distributions from the grid of stellar models of Kurucz (1993). The model atmosphere has been extended outwards by adopting a suitably scaled solar chromosphere as in T97. For $\log \tau_5 \lesssim -4$ (where $\tau_5$ is the optical depth at 5000 Å), the temperature of the stellar model, $T^\star(\tau_5)$, is given by $T^\star(\tau_5) = T^\odot(\tau_5) \cdot T^\star_{\rm eff}/T^\odot_{\rm eff}$, where $T^\odot(\tau_5)$ is taken from the solar reference model of Maltby et al. (1986), and $T^\star_{\rm eff}$ and $T^\odot_{\rm eff}$ are the stellar and solar effective temperatures, respectively. The electron density $N_{\rm e}$ in the chromosphere was assumed to be constant and equal

to its photospheric value at $\log \tau_5 = -4$. This simplification is justified by the very low sensitivity of the equivalent width to $N_e$ in our cool non-active stars (see T97), and by the relatively slow variation of $N_e$ in chromospheres (Ayres 1979). The models resulting from this approach are similar to those plotted in Figs. 1 and 2 of T97, but about 200 K hotter in the photosphere.

For all the models of the grid, we have adopted the microturbulence height distribution from the solar semi-empirical model. Actually, microturbulence only affects the Gaussian core of the K I and Na I D lines, while it leaves the wings unaltered. Therefore, the effect of a different microturbulence – e.g. lower in dwarf and stronger in giant stars – on the equivalent widths of these lines, which have well developed wings, is negligible (see T97).

### *3.2. Spectral line synthesis*

For the NLTE synthesis of the Na I D and K I lines over the grid of model atmospheres, we used version 2.2 of the code MULTI, implemented by Carlsson (1986). This version of the code adopts a variety of continuum opacity sources, including the opacity due to the formation of a number of diatomic molecular lines, calculated by the program described by Gustafsson (1973) and Gustafsson et al. (1975). Moreover it allows for the inclusion of background opacity from lines by filling a suitable line data file as well as by using an explicit wavelength dependent analytical formula. We used the second option in this work, and our additional opacity prescription is illustrated in Sect. 3.3. The potassium model atom contains 13 levels, 20 lines and 12 bound-free transitions. The sodium model atom contains 11 levels, 24 lines and 10 bound-free transitions. These models are based on the works of Caccin et al. (1993), Bruls et al. (1992) and Andretta et al. (1997).

For the Na and K abundances, we used the meteoritic values $\log N(\mathrm{Na}) = 6.31$ and $\log N(\mathrm{K}) = 5.13$ (in the logarithmic scale where hydrogen abundance is 12), given by Grevesse & Anders (1991).

### *3.3. Additive opacity*

We added to the standard background opacity present in the version 2.2 of MULTI a term scaled on the $H^-$ (bound-free + free-free) opacity coefficient, defined as

$$\kappa_{\mathrm{add}}(\lambda, z) = q(\lambda) \cdot OF \cdot \kappa_{\mathrm{H^-}}(\lambda, z); \quad (2)$$

$q(\lambda)$ is inferred from the opacity enhancement factor introduced by Zwaan (1974) to match the observed continuum intensity of sunspots, and has the expression

$$q(\lambda) = \begin{cases} 1.7 - 10^{-4}\,(\lambda - 5000) & \text{if } 5000\text{Å} < \lambda < 7000\text{Å} \\ 1.5\text{–}2.5\,10^{-4}\,(\lambda - 7000) & \text{if } 7000\text{Å} < \lambda < 9000\text{Å} \\ 1 & \text{otherwise;} \end{cases} \quad (3)$$

$OF$ represents a further multiplicative opacity factor that we have introduced in order to fit our observations of M-type dwarf stars; $\kappa_{\mathrm{H^-}}(\lambda, z)$ is the wavelength and depth dependent $H^-$ (b-f + f-f) opacity coefficient.

**Table 2.** Stellar parameters adopted in the calculation of the $W_K$ vs. $T_{\mathrm{eff}}$ relations for dwarf and giant stars (see Figs. 2 and 3). The units for $T_{\mathrm{eff}}$ and $g$ are K and cm s$^{-2}$, respectively.

| DWARFS | | GIANTS | |
|---|---|---|---|
| $T_{\mathrm{eff}}$ | $\log g$ | $T_{\mathrm{eff}}$ | $\log g$ |
| 3500 | 4.5 | 3500 | 1.0 |
| 3750 | 4.5 | 3750 | 1.5 |
| 4000 | 4.5 | 4000 | 2.0 |
| 4250 | 4.5 | 4250 | 2.0 |
| 4500 | 4.5 | 4500 | 2.5 |
| 4750 | 4.5 | 4750 | 3.0 |
| 5000 | 4.5 | 5000 | 3.0 |
| 5250 | 4.5 | 5250 | 3.0 |
| 5500 | 4.5 | 5500 | 3.5 |
| 5750 | 4.5 | 5750 | 3.5 |
| 6000 | 4.5 | 6000 | 3.5 |
| 6250 | 4.5 | 6250 | 3.5 |
| 6500 | 4.5 | 6500 | 3.5 |

## 4. Results

### *4.1. Calculated $W_K$ vs. $T_{\mathrm{eff}}$ and $\log g$*

We have calculated $W_K$, with and without additional opacity, for solar metallicity ([Fe/H]= 0.0), and for a grid of values of $T_{\mathrm{eff}}$ and $\log g$ representing dwarf and giant stars. The grid is given in Table 2, and has been derived from Gray (1989). The computed $W_K$ vs. $T_{\mathrm{eff}}$ relations for models with no additional opacity ($OF$=0.0) and with additional opacity ($OF$=1.5) are plotted in Figs. 2 and 3, for dwarfs and giants, respectively.

Fig. 2 shows that for the hottest dwarfs of the sample the models with $OF$=0.0 are able to reproduce the observations, while for smaller $T_{\mathrm{eff}}$ this is possible only if $OF$ is about 1.5. The observed data do not allow to assess whether there is a continuous or an abrupt change between $OF$=0.0 at large $T_{\mathrm{eff}}$ and $OF$=1.5 at low $T_{\mathrm{eff}}$. However, the opacity model appears to be able to reproduce the entire range of the observed $W_K$ for $OF$ spanning these values. Fig. 3 shows that a smaller amount of opacity, compared to dwarfs, has to be added to the models in order to reproduce the observations for giant stars at intermediate values of $T_{\mathrm{eff}}$. On the other hand, at low $T_{\mathrm{eff}}$ the model is insufficient, and many observed values of $W_K$ are even greater than the corresponding values computed without additional opacity. This fact, which indicates that the alkali resonance lines in giants deserves special care, has induced us to focus our attention only on dwarf stars when comparing the observed and computed profiles (Sect. 4.2).

In the atmospheres of M dwarfs, the Van der Waals interaction is the dominant broadening mechanism (e.g. Schweitzer et al. 1996). Therefore, in order to investigate another possible cause for the discrepancy found in T97, we have tested the sensitivity of $W_{\mathrm{Na}}$ to variations in the Van der Waals broadening. We find that the decrease of $W_{\mathrm{Na}}$ necessary to fit the observations could be obtained only by decreasing the Van der Waals damping constant by a factor 2, which is obviously not accept-

**Table 3.** Subsample of the observed M dwarf stars. $W_{\rm K}$ and $W_{\rm Na}$ are the measured equivalent widths (in Å) of the KI and NaI D lines, respectively.

| HD # | Gl # | $T_{\rm eff}$ | $\log g$ | [Fe/H] | $W_{\rm K}$ | $W_{\rm Na}$ |
|---|---|---|---|---|---|---|
| 209290 | 846 | 3750[a] | 5.0[c] | $-1.5$[c] | 0.85 | 10.0 |
| | | 3640[b] | | | | |
| | | 3580[c] | | | | |
| 42581 | 229 A | 3814[c] | 5.0[c] | 0.0[c] | 0.92 | 9.4 |
| | | 3630[d] | | | | |
| 36395 | 205 | 3737[c] | 5.0[c] | $-1.5$[c] | 0.98 | 10.0 |
| | | 3625[e] | 4.8[e] | $+0.6$[e] | | |
| | | 3400[f] | | 0.0[g] | | |
| 131976 | 570 B | 3506[h] | 4.73[i] | 0.09[j] | 0.99 | 9.9 |
| 119850 | 526 | | | 0.01[j] | 0.85 | 8.7 |

[a] Based on the $T_{\rm eff}$ vs. spectral type calibration of Ali et al. (1995)
[b] Ali et al. (1995)
[c] Alonso et al. (1996)
[d] Schiavon et al. (1997), based on the $(R-I)_{\rm Cousins}$ vs. $T_{\rm eff}$ calibration of Bessel (1991)
[e] Cayrel de Strobel et al. (1992)
[f] Neff et al. (1995), based on Bessel (1991)
[g] Serote Roos et al. (1996)
[h] Worthey et al. (1994), based on the $T_{\rm eff}$ calibration of Johnson (1966)
[i] Gorgas et al. (1993)
[j] Based on the empirical relation of Eggen (1996)

able, since this parameter is known with a high precision for the alkali resonance lines (Allende Prieto et al. 1997).

### *4.2. Comparison between observations and calculations for selected M dwarf stars*

The agreement between observed and calculated equivalent widths, obtained for M dwarf stars when the additional background opacity is included, has induced us to extend our analysis to the line profiles. In fact, we restricted ourselves to reproduce the general shape of the observed profiles, since we are well aware that a detailed fit needs a more accurate model of the background additional opacity, as stressed for example by Short & Doyle (1998).

We have compared the observed and computed profiles of the Na I D and K I lines for a subsample of 5 dwarf stars with spectral type in the range M0.5-M1.5; these stars span a narrow $T_{\rm eff}$ range, comparable to the typical uncertainty on the effective temperatures of early-M dwarfs.

In Table 3 we report the fundamental parameters deduced from the literature for these stars, together with our measurements of $W_{\rm K}$ and $W_{\rm Na}$. Note that the mean uncertainty on $T_{\rm eff}$ is also comparable to the step of our grid of atmospheric models, i.e. $250$K. Furthermore, the empirically determined $\log g$ ranges between 4.7 and 5.0, and therefore we have adopted the range 4.5–5.0 for constructing the stellar atmospheric models. Moreover, [Fe/H]= 0 for almost all the stars in Table 3; only HD209290 and HD36395 are reported as low metallicity stars by Alonso et al. (1996). However, Cayrel de Strobel et al. (1992) classify HD36395 as a super metal rich star with [Fe/H]=0.6, while Serote Roos et al. (1996) indicate that probably this high value is due to the weak intensity of the hydrogen lines. Therefore we have used solar metallicity also for HD36395. The K I and Na I D profiles observed for the stars in Table 3 are shown in Figs. 4 and 5, respectively. From Fig. 5 it is apparent that the Na I D profile of HD209290 is disturbed by many more lines than the other stars in Table 3. In particular, most of the strong lines present on the Na I D spectrum are telluric lines of water vapour (see for example Lundström et al. 1991). In fact, HD209290 is the only star in Table 3 which has been observed at the McDonald telescope, and not at La Silla. Therefore, its spectrum has been obtained under very different terrestrial atmospheric conditions.

Let us neglect the low metallicity star HD209290 for the moment, and focus our attention on the remaining stars. In order to investigate the effect of the uncertainties in the model parameters of these stars, we have computed the profiles of the K I and Na I D lines over a grid of atmospheric models with $T_{\rm eff} = 3500$K, $3750$K, $\log g = 4.5$dex, $5.0$dex, [Fe/H] = 0.0, and with several values for the opacity factor $OF$.

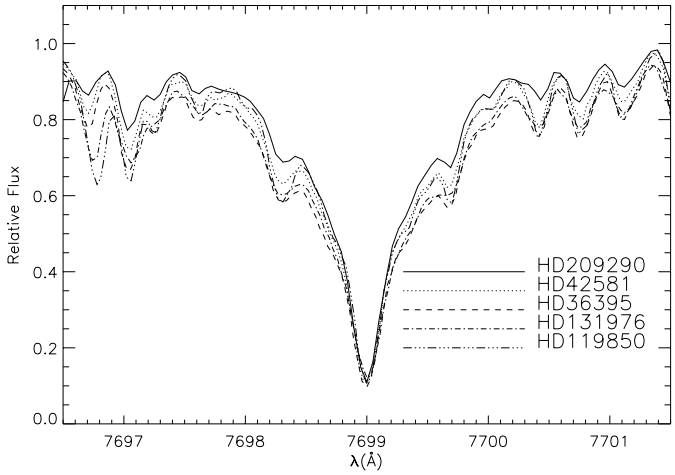


**Fig. 4.** K I profile for stars in Table 3.

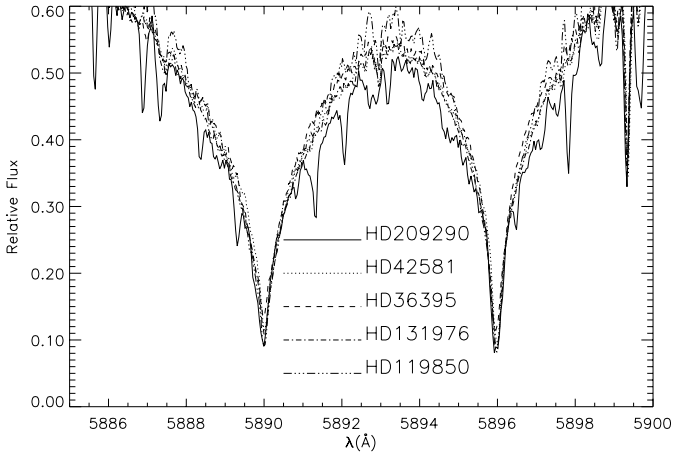


**Fig. 5.** Na I profile for stars in Table 3.

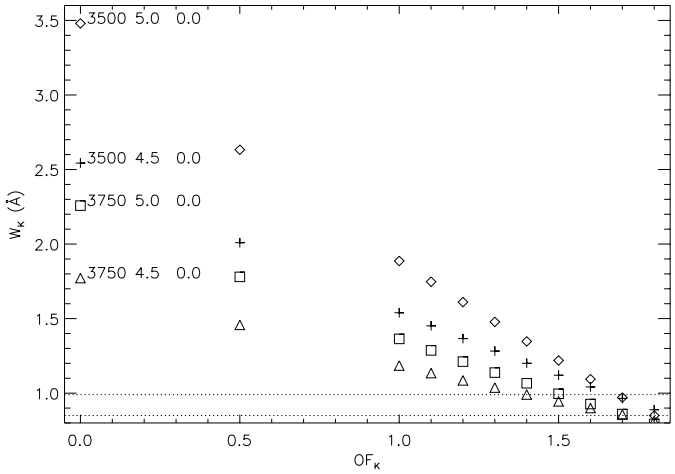


**Fig. 6.** Computed $W_{\rm K}$ vs. $OF$ for models with additional opacity. Each symbol refers to a set of values of $T_{\rm eff}$, $\log g$, and [Fe/H], indicated in this order on the left side of the plot. The dotted lines represent upper and lower limits for the observed $W_{\rm K}$ (Table 3).

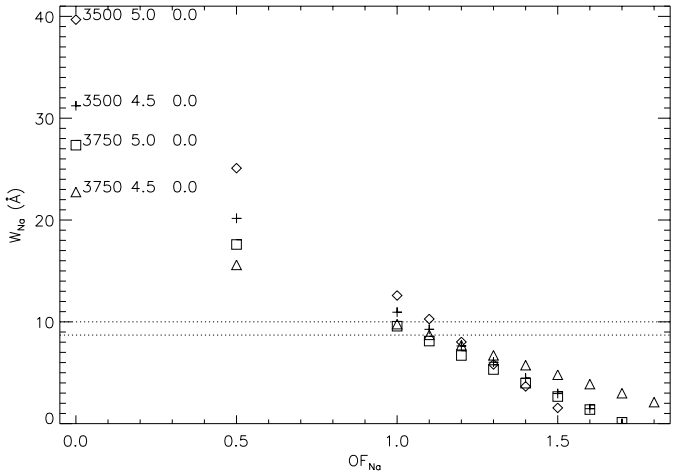


**Fig. 7.** Same as Fig. 6, but for Na I.

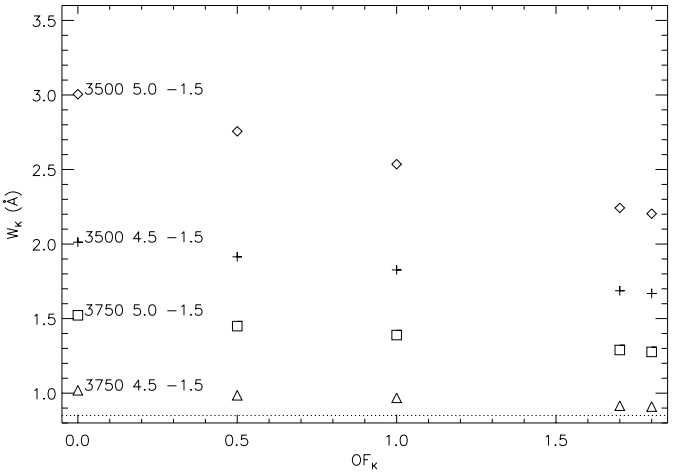


**Fig. 8.** Computed $W_{\rm K}$ for models with [Fe/H]=$-1.5$ ($T_{\rm eff}$ and $\log g$ as in Fig. 6). The dotted line represents the observed $W_{\rm K}$ for HD209290.

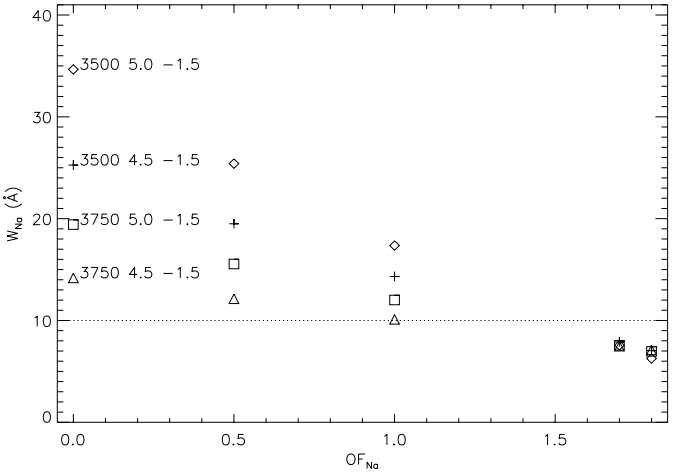


**Fig. 9.** Same as Fig. 8, but for Na I.

The observed $W_{\rm K}$ and $W_{\rm Na}$ span the ranges from 0.85 to 0.99 Å, and from 8.7 to 10.0 Å, respectively. These lower and upper limits are plotted as dotted lines in Figs. 6 and 7. These figures show the trend of the computed $W_{\rm K}$ and $W_{\rm Na}$ vs. $OF$. It is clear that none of the models is able to reproduce $W_\lambda$ if no additional opacity is included, while $OF \geq 1.0$ reduces substantially the discrepancy between the computed and observed equivalent widths. In particular, all the models of the grid produce $W_{\rm K}$ = 0.85–0.99 Å for $OF_{\rm K}$ = 1.3–1.8, and $W_{\rm Na}$ = 8.7–10.0 Å for $OF_{\rm Na} = 0.95$–1.20.

For the metal-poor star HD209290, we have repeated the calculations over the same grid of atmospheric models, but with [Fe/H]=$-1.5$. The same logarithmic decrease has been applied to the Na and K abundances, as well as to the abundances of the elements taken into account by MULTI in calculating the continuum opacity. In general, $W_{\rm K}$ and $W_{\rm Na}$ are less sensitive to the additional opacity for large $T_{\rm eff}$ and low $\log g$ (see Figs. 6 and 7). On the other hand, Figs. 8 and 9 show that, at low metallicity ([Fe/H]=$-1.5$), this sensitivity is even weaker; in fact, for $T_{\rm eff}$ = 3750K and $\log g = 4.5$, $W_{\rm K}$ is almost constant with $OF_{\rm K}$. Note also that the effect of a factor $OF = 1$ in the additional opacity is in general greater than the effect due to a variation $\Delta$[Fe/H]= $-1.5$ in metallicity, while these two effects become comparable for increasing $T_{\rm eff}$ and decreasing $\log g$.

In general, the amount of additional opacity necessary to reproduce $W_{\rm Na}$ is less model dependent than that for the K I line. Therefore, we have used the K I line to choose the best atmospheric model in the grid, by comparing the computed and observed K I line profiles, and then we have evaluated $OF_{\rm K}$ and $OF_{\rm Na}$ for each star. For instance, the atmospheric model for HD42581 has been selected on the basis of a comparison between the observed K I line profile and the profiles computed with $T_{\rm eff}$= 3500 and 3750 K, $\log g$= 4.5 and 5.0, [Fe/H]= 0.0 (Fig. 10). Of course, a better fit could be reached at this stage if we let the atmospheric parameters vary on larger ranges; however, we used the parameter values, listed in Table 4 and derived from literature, to constrain our atmospheric models. Af-

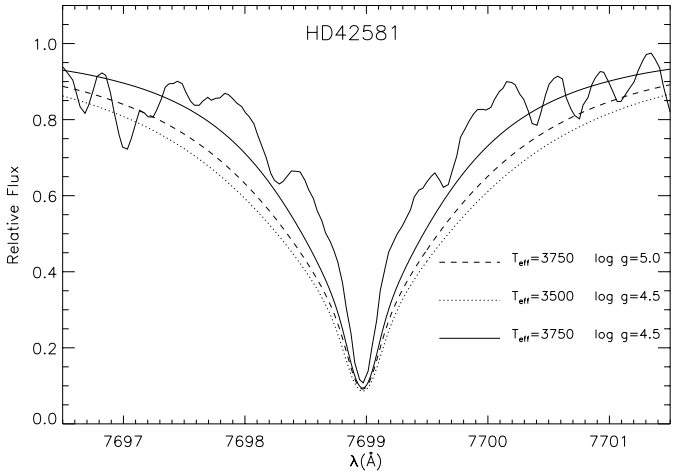


**Fig. 10.** K I $\lambda$7699 profiles for HD42581; solid thick line refers to the observed profile; other line types refer to profiles calculated with different values of $T_{\rm eff}$ and $\log g$, as indicated in the figure; all computed profiles correspond to solar metallicity and no additional opacity, and have been convolved with a Gaussian ($\Delta\lambda = 130$mÅ) instrumental profile.

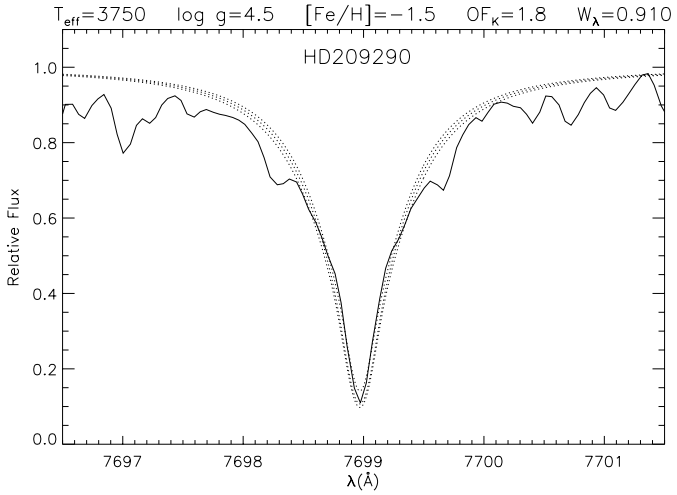


**Fig. 11.** Observed (solid line) and computed K I $\lambda$7699 profiles for HD209290; the parameters of the best fit are given on top of the plot; the dotted lines represent the profiles computed with $OF_{\rm K}$= 0.0, 1.0 and 1.8, starting from the broadest one; these have been convolved with a Gaussian ($\Delta\lambda = 130$mÅ) instrumental profile.

**Table 4.** Model parameters for the M dwarf stars. $OF_{\rm K}$ and $OF_{\rm Na}$ are the additive opacity factors adopted to fit the observed K and Na spectra, respectively. $W_{\rm K}$ and $W_{\rm Na}$ are the computed equivalent widths (in Å).

| HD # | $T_{\rm eff}$ | $\log g$ | [Fe/H] | $OF_{\rm K}$ | $OF_{\rm Na}$ | $W_{\rm K}$ | $W_{\rm Na}$ |
|---|---|---|---|---|---|---|---|
| 209290 | 3750 | 4.5 | −1.5 | 1.8 | 1.0 | 0.91 | 10.1 |
| 42581 | 3750 | 4.5 | 0.0 | 1.5 | 1.0 | 0.94 | 9.8 |
| 36395 | 3750 | 4.5 | 0.0 | 1.4 | 1.0 | 0.99 | 9.8 |
| 131976 | 3750 | 4.5 | 0.0 | 1.4 | 1.0 | 0.99 | 9.8 |
| 11985 | 3750 | 4.5 | 0.0 | 1.7 | 1.1 | 0.86 | 8.7 |

terwards, an improved fit of the observed line profile has been obtained by the inclusion of the additional background opacity.

The results of this approach are listed in Table 4; the computed and observed profiles for HD209290 are shown in detail in Figs. 11 and 12. Those for HD42581, which is representative of our solar metallicity M dwarfs, are plotted in Figs. 13 and 14. Note that, to better reproduce the observing conditions, all the computed profiles in these plots have been convolved with a Gaussian instrumental profile having width $\Delta\lambda = 130$ and 100 mÅ for K I and Na I, respectively. The comparison of Figs. 11 and 12 with Figs. 13 and 14 shows that, in general, the sensitivity of the computed profiles to the additional opacity is smaller for atmospheric models with lower metallicity, and in particular that, for [Fe/H]= $-1.5$, the computed K I line profile is almost insensitive to $OF_{\rm K}$. We need to add a smaller opacity factor $OF$ in order to fit the Na I D lines ($OF_{\rm Na} \sim 1.0$), with respect to the K I line ($OF_{\rm K} \sim 1.5$). According to the definitions given above, this implies that the additive opacity in units of $H^-$ opacity, i.e. the product $OF \cdot q(\lambda)$, should be almost constant with $\lambda$.

Note that a compromise has to be accepted in reproducing the general shape of the Na I D lines, because the computed

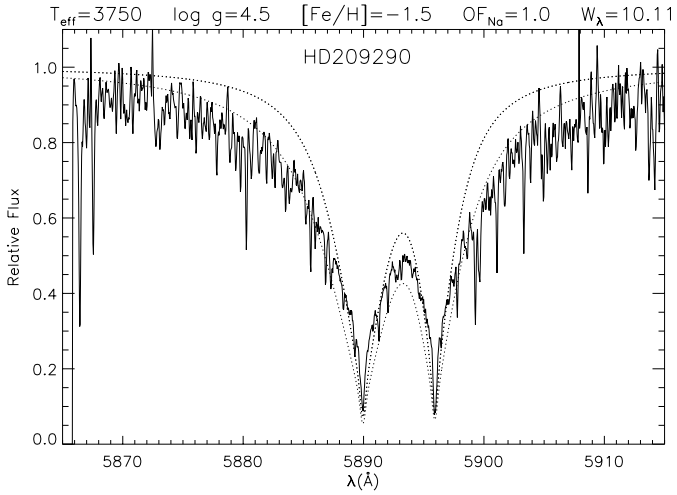


**Fig. 12.** Observed (solid line) and computed Na I $\lambda$7699 profiles for HD209290; the parameters of the best fit are given on top of the plot; the dotted lines represent the profiles computed with $OF_{\rm K}$= 0.0 and 1.0, starting from the broadest one; these have been convolved with a Gaussian ($\Delta\lambda = 100$mÅ) instrumental profile.

cores are generally too broad and the wings too weak. We are not able to state the precise reasons for this further discrepancy between observations and calculations. However a number of effects, not included in our present approach, needs to be investigated in more detail. For instance, a more realistic model for the background opacity including lines in detail, the uncertainty on the temperature gradient throughout the atmospheres of such highly convective stars (Bernkopf 1998) and the effect of velocity fields of different spatial scales on the line profile are all issues which deserve quantitative study.

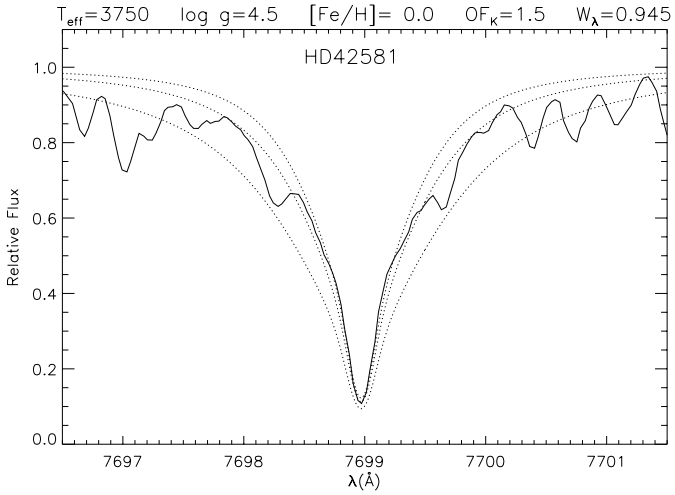


**Fig. 13.** Observed (solid line) and computed K I $\lambda$7699 profiles for HD42581; the parameters of the best fit are given on top of the plot; the dotted lines represent the profiles computed with $OF_{\rm K}$= 0.0, 1.0 and 1.5, starting from the broadest one; these have been convolved with a Gaussian ($\Delta\lambda = 130$mÅ) instrumental profile.

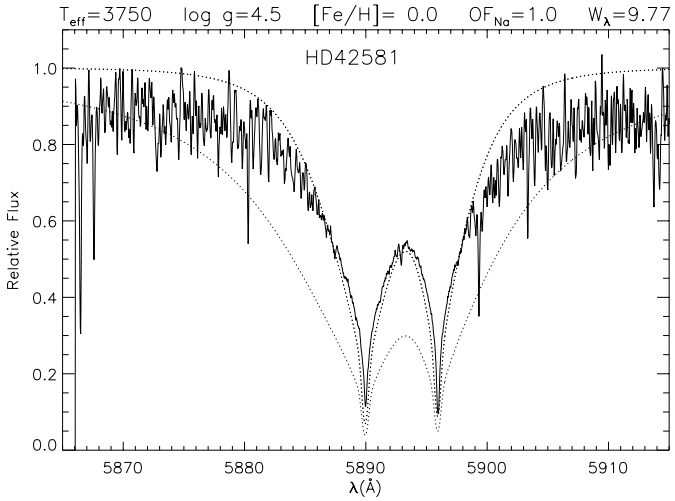


**Fig. 14.** Observed (solid line) and computed Na I D profiles for HD42581; the parameters of the best fit are given on top of the plot; the dotted lines represent the profiles computed with $OF_{\rm K}$= 0.0 and 1.0, starting from the broadest one; these have been convolved with a Gaussian ($\Delta\lambda = 100$mÅ) instrumental profile.

## 5. Conclusions

We have measured the equivalent width $W_{\rm K}$ of the K I resonance line at 7699 Å for 32 dwarf and 41 giant stars with $T_{\rm eff}$ spanning the intervals between 3500 and 6500 K, and 3600 and 5400 K, respectively. We have presented two weighted third order polynomial fits for the corresponding $W_{\rm K}$ vs. $T_{\rm eff}$ relations. These relations can be inverted and used to determine $T_{\rm eff}$ with a dispersion of about $\pm$200 K, the sensitivity being higher for dwarf stars than for giants.

We have computed $W_{\rm K}$ for dwarf and giant cool stars, finding that, the models without additional opacity do not reproduce the observations at low $T_{\rm eff}$. This result is similar to that found for $W_{\rm Na}$ in T97. In particular, for dwarf stars with $T_{\rm eff} \lesssim$ 4000 K, the observed $W_{\rm K}$ is overestimated by the line synthesis, while for giant stars cooler than about 3800 K it is generally underestimated, which indicates that further investigation should be carried out for giants. Therefore, we have focussed our attention on dwarf stars, explaining the overestimation of $W_{\rm K}$ in terms of a missing opacity which has to be added to the continuum opacity when $T_{\rm eff}$ is sufficiently low. This kind of opacity is easily produced by the huge amount of neutral atomic and molecular absorption lines present in the spectra of the coolest stars. The additional opacity tends to lower the local absolute continuum flux, and it also affects the absolute line intensity, especially in the wings where the continuum opacity relative to the line opacity is larger (see Andretta et al. 1997 and also Falchi & Mauas 1998). The resulting effect is that the alkali resonance lines reach more quickly the continuum, and therefore their equivalent widths decrease.

By means of a simple prescription, consistent with radiative transfer, we have estimated the amount of background opacity missing from the adopted models, and necessary to fit the general shape of the Na I D and K I $\lambda$7699 features in a sample of M dwarf stars. However, we stress that a treatment of opacity more accurate than ours is necessary in order to produce model line profiles fitting observations in detail (e.g. Short & Doyle 1998 and references therein). We do not add opacity in the UV range, because we expect that adding opacity in this spectral range would not change significantly our results. In fact, while in the solar case the Na I D lines are dominated by the photoionization processes in the UV from the ground state to the continuum, in the M dwarf stellar atmospheres the UV radiation field is much less intense than in the sun, so that probably these lines are collisionally controlled (Andretta et al. 1997). Moreover, for the K I line, photoionization processes in the UV are not very important even in the sun (Bruls et al. 1992).

Furthermore, we have verified that the discrepancy between observations and calculations without additional opacity cannot be ascribed to the uncertainty on the Van der Waals damping constant. However, the line broadening also depends on the density of neutral hydrogen, which in turn reflects the uncertainties on the temperature distribution and on the kind of state equation used to build the model. For example, at an optical depth of about $-0.1$, this density in one of our models ($T_{\rm eff}$= 3750 K, $\log g$= 4.5, [Fe/H]= 0.0) is about a factor 1.5 the H I density in the model of Allard & Hauschildt (1995) with $T_{\rm eff}$= 3700 K, $\log g$= 4.5, and [Fe/H]= 0.0. This means that probably a minor amount of opacity would have been necessary to reproduce our observations of M dwarfs, if the latter atmospheric models had been adopted.

Finally, we note that in this work we have dealt only with relative profiles. However, because line blanketing strongly affects the measured values of the absolute continuum flux, spectrophotometric observations of the continuum flux in the neighbourhood of the alkali resonance lines for the stars of our sample, compared with the calculated continuum and line fluxes, would give an important constraint on the amount of missing opacity.

*Acknowledgements.* We thank J.M. Alcalà for providing us with his MIDAS procedures for spectroscopic data reduction, for helping us in the preparation of the second observing run at ESO-CAT, and for many useful suggestions concerning the data analysis, V. Andretta for his stimulating comments on the model calculations, and the anonymous referee for helping us to put the paper in the right perspective.

## References

Ali B., Carr J.S., Depoy D.L., Frogel J.A., Sellgren K., 1995, AJ 110, 2415
Allard F., Hauschildt P.H., 1995, ApJ 445, 433
Allard F., Alexander D.R., Hauschildt P.H., 1997, Model Atmospheres: Brown Dwarfs from the Stellar Perspective, invited talk in Brown Dwarfs and Extrasolar Planets, International Workshop, March 17–21, 1997, Puerto de la Cruz, Tenerife, Spain
Allende Prieto C., García López R.J., Trujillo Bueno J., 1997, ApJ 483, 941
Alonso A., Arribas S., Martinez-Roger C., 1996, A&AS 117, 227
Andretta V., Doyle J.C., Byrne P.B., 1997, A&A 322, 266
Avrett, E.H., Machado M.E., Kurucz R.L., 1986, In: Neidig D.F. (ed.) The Lower Atmosphere in Solar Flares. p. 216
Ayres T.R., 1979, ApJ 228, 509
Bernkopf J., 1998, A&A 332, 127
Bessel M.S., 1991, AJ 101, 662
Bruls J.H.M.J., Rutten R.J., Shchukina N.G., 1992, A&A 265, 237
Brynildsen N., Engvold O., Hansteen V., Brault J.W., 1993, private communication
Carlsson M., 1986, A Computer Program for Solving Multi-Level Non-LTE Radiative Transfer Problems in Moving or Static Atmospheres, Report No. 33, Uppsala Astronomical Observatory
Cayrel de Strobel G., Hauck B., Francois P., et al., 1992, A&AS 95, 273
Caccin B., Gomez M.T., Severino G., 1993, A&A 276, 219
Eggen O.J., 1996, AJ 111, 466
Falchi A., Mauas J.D., 1998, A&A, in press
Gorgas J., Faber S.M., Burstein D., et al., 1993, ApJS 86, 153
Gray D.F., 1989, In: Cram L.E., KuhiL.V. (eds.) FGK Stars and T Tauri Stars. Monograph Series on nonthermal phenomena in stellar atmospheres, NASA SP–502, p. 7
Gray D.F., 1992, In: The observation and analysis of stellar photospheres. 2$^{nd}$ edition, Cambridge University Press, p. 391
Grevesse N., Anders E., 1991, In: Cox A.N., Livingston W.C., Matthews M.S. (eds.) Solar Interior and Atmosphere. p. 1227
Gustafsson B., 1973, Uppsala Astr. Obs. Ann., Band 5, No. 6
Gustafsson B., Bell R.A., Eriksson K., Nordlund Å., 1975, A&A 42, 407
Johnson H.L., 1966, ARA&A 4, 193
Kaper L., Pasquini L., 1996, ESO Operating Manual, 3p6CAT-MAN-0633-0001
Kurucz R.L., 1991, In: Davis Philip A.G., Upgren A.R., Jancs K.A. (eds.) Precision Photometry: Astrophysics of the Galaxy. L. Davis Press, Schenectady
Kurucz R.L., 1993, ATLAS9 stellar atmospheres programs and 2 Km/s grid, CD-ROM No. 18
Lundström I., Ardeberg A., Maurice E., Lindgren H., 1991, A&AS 91, 199
Maltby P., Avrett E.H., Carlsson M., et al., 1986, ApJ 306, 284
Mauas P.J.D., Falchi A., Pasquini L., Pallavicini R., 1997, A&A 326, 249
Montes D., Martin E.L., 1998, A&AS 128, 485
Neff J.E., O'Neal D., Saar S.H., 1995, ApJ 452, 879
Schiavon R.P., Barbuy B., Rossi S.C.F., Milone A., 1997, ApJ 479, 902
Schweitzer A., Hauschildt P.H., Allard F., Basri G., 1996, MNRAS 283, 821
Serote Roos M., Boisson C., Joly C., 1996, A&AS 117, 93
Severino G., Gomez M. T., Caccin B., 1994, Solar Surface Magnetism. NATO ASI Series C433, 169
Short C.I., Doyle J.C., 1997, A&A 326, 287
Short C.I., Doyle J.C., 1998, A&A 336, 613
Tripicchio A., Severino G., Covino E., Terranegra L., García López R.J., 1997, A&A 327, 681
Uesugi A., Fukuda I., 1982, Catalogue of stellar rotational velocities (revised). University of Kyoto, Department of Astronomy
Worthey G., Faber S.M., Gonzalez J.J., Burstein D., 1994, ApJS 94, 687
Zwaan C., 1974, Sol. Phys. 37, 99